Generation of Feasible Gripper Trajectories in Automated Composite Draping by means of Optimization

Krogh, Christian; Sherwood, James A.; Jakobsen, Johnny

Published in:
Advanced Manufacturing: Polymer and Composites Science

DOI (link to publication from Publisher):
10.1080/20550340.2019.1699691

Publication date:
2019

Document Version
Publisher's PDF, also known as Version of record

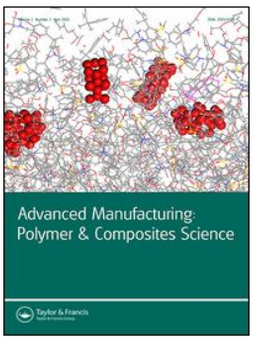

Taylor & Francis
Taylor & Francis Group

Advanced Manufacturing: Polymer & Composites Science

ISSN: 2055-0340 (Print) 2055-0359 (Online) Journal homepage: https://www.tandfonline.com/loi/yadm20

Generation of feasible gripper trajectories in automated composite draping by means of optimization

Christian Krogh, James A. Sherwood & Johnny Jakobsen

To cite this article: Christian Krogh, James A. Sherwood & Johnny Jakobsen (2019) Generation of feasible gripper trajectories in automated composite draping by means of optimization, Advanced Manufacturing: Polymer & Composites Science, 5:4, 234-249, DOI: 10.1080/20550340.2019.1699691

To link to this article: https://doi.org/10.1080/20550340.2019.1699691

Published online: 17 Dec 2019.

ADVANCED MANUFACTURING: POLYMER & COMPOSITES SCIENCE
2019, VOL. 5, NO. 4, 234–249
https://doi.org/10.1080/20550340.2019.1699691

Generation of feasible gripper trajectories in automated composite draping by means of optimization

Christian Krogh[a], James A. Sherwood[b] and Johnny Jakobsen[a]

[a]Department of Materials and Production, Aalborg University, Aalborg East, Denmark; [b]Department of Mechanical Engineering, University of Massachusetts, Lowell, Lowell, MA, USA

ABSTRACT

Prepreg composites find great applicability in e.g. the automotive and aerospace industries. A major challenge with this class of material systems is the accurate placement of a fabric that can be very tacky and hence sticks to the mold surface. In this study, automatic draping of entire plies of woven prepregs is considered. A robot end effector with a grid of actuated grippers is under development and it has the ability to position the plies onto double-curved mold surfaces of low curvature. The key issue is how the grippers of the end effector should move to achieve successful drapings of the plies that meet the quality requirements of the industry. In this study, an approximate ply model based on cables with bending stiffness is applied in an optimization framework where the gripper movements constitute the design variables. The optimization framework has taken inspiration from manual layup procedures. The numerical draping results indicate the usefulness of the cable model used in connection with the optimization framework. The next step is to implement the generated gripper trajectories on the physical robot system.

GRAPHICAL ABSTRACT

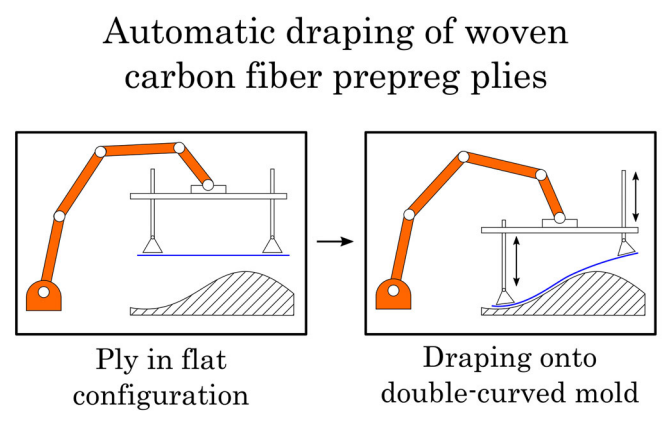

ARTICLE HISTORY
Received 5 November 2019
Accepted 15 November 2019

KEYWORDS
Woven prepreg; draping; trajectory optimization; offline motion planning; automation

1. Introduction

Although composites exhibit properties that are very desirable from a mechanical point of view, a major drawback is the cost associated with their manufacturing, which is dominated by manual steps, e.g. hand placement of plies. To this end, significant research efforts are being pursued for lowering the manufacturing cost by utilizing robots [1]. In the *FlexDraper* research project [2], a robot end effector with an array of actuated grippers is employed to manipulate entire woven prepreg plies onto double-curved mold surfaces of low curvatures. Prepreg plies comprise a fabric which is pre-impregnated with resin. This operation constitutes an automatic draping process that can directly replace the manual hand layup.

A key issue related to the automation of the draping process, is the concept of *draping strategies* which for the robot system translates to its gripper trajectories. Handling of the prepreg ply by the FlexDraper robot system was previously studied by means of a nonlinear, rate-dependent finite element (FE) model [3]. It was found that the end result is highly dependent on the gripper paths and that

CONTACT Christian Krogh ck@mp.aau.dk Department of Materials and Production, Aalborg University, Aalborg East, Denmark

wrinkles can easily form during draping. In an industrial context, it is essential to avoid wrinkling.

The manufacturing of composite preforms with a punch, die and blank holder is a common operation in e.g. the automotive industry. To this end, the pressure created by the blank holder over the course of the process cycle has been subject to optimization with the purpose of avoiding wrinkling [4, 5]. Recently, the concept of a multi-punch tool with individually controllable segments has also been investigated [6].

Concerning composite layup on a mold surface, a number of research groups have been studying automation of the process and the concept of draping sequences. Eischen and Kim [7] considered the automatic placement of a strip of apparel fabric on a flat surface. By means of optimization the authors generated manipulator paths that minimized the reaction force. In the work by Reinhart and Ehinger [8], a robot end effector in the form of an elastic roller with suction was used to drape carbon-fiber preforms for subsequent resin infusion. The authors discussed different *draping strategies* for a number of molds, i.e. rolling motions of the tool in different directions. Molfino et al. [9] outlined a *handling strategy* for use with a robot system which relies on a 3 D laser scanner. The laser scanner was used to identify placing strategies on the mold for dry fabric. Nagele et al. [10] presented a *backward-oriented* approach for offline programming of the draping process of dry fabrics for a system with a grid of grippers. The idea is to start from the draped configuration and then determine robot sequences to some starting point. It is, however, not clear how well the approach can take the path-dependency of the prepreg ply into account.

Catenary models have been explored by some researchers for representing the ply behavior. Flixeder et al. [11] developed a force-based control system for handling of dry 2 D fabrics, where the manipulator movements are generated online using a catenary model. A catenary model was also used by Eckardt et al. [12] for the purpose of finding the inclination of the grippers which will not induce any unnecessary bending in the dry fabric. In their paper, the authors also discussed the use of a *seed point* or *seed curve* from where the draping can start, which originates from manual layup. They investigated three manually created draping strategies on a single-curved demonstrator part. The first two draping strategies were rejected due to induction of defects while the third was successful.

Brinker et al. [13] discussed *drape paths* and presented a figure with discrete gripper trajectories arising from a kinematic drape simulation. Newell and Khodabandehloo [14] presented a large deflection beam model for draping automation and experimentally validated it against a strip of prepreg. Also, a large-deflection shell model was introduced by Lin et al. [15] for real time ply prediction under certain pre-defined boundary conditions.

The references mentioned above all provide inspiration for the work presented in this paper but the methods are not directly applicable to draping of prepreg fabric on arbitrary 3 D molds with the particular robot tool considered in this study. The goal of the current study is to generate feasible draping sequences, i.e. off-line gripper trajectories, for the robot of the FlexDraper project. The generation must be done automatically. Here, a computationally efficient fabric model based on cables with bending stiffness is employed to predict the mechanical behavior of the prepreg ply during draping. The trajectories are generated by means of an optimization scheme which incrementally moves the grippers based on the predicted ply response. The rest of the paper is organized as follows: Section 2 provides a detailed description of the problem to be solved and the robot tool. Section 3 introduces the cable fabric model and discusses its properties. Section 4 presents the optimization scheme and Section 5 presents numerical results. Finally, a discussion and a conclusion complete the paper.

2. Problem description

The production of prepreg composites comprises a series of steps as outlined in Figure 1. This study focuses on the draping step but the high production costs could be addressed in a number of other ways.

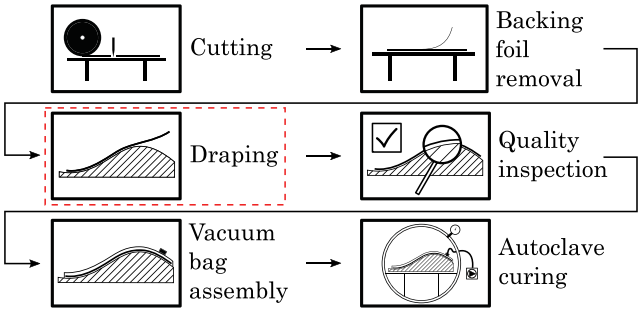

Figure 1. The major steps in the production of prepreg composites. This paper concerns the draping step.

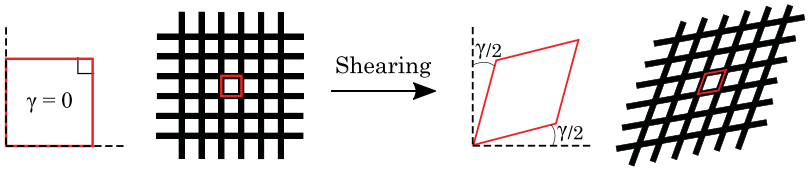

Figure 2. Fabric shear involving fiber tows rotating at the cross-over points. γ is the shear angle.

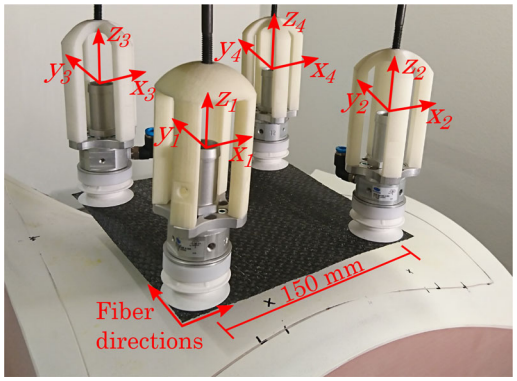

Figure 3. The concept of the robot end effector under development with a 2 × 2 grid of x, y, z controllable suction cups. The prepreg ply is held above the mold.

Another costly step is for instance the curing in an autoclave which requires a significant amount of time and energy. Autoclave curing is usually employed for small-batch production in the aerospace industry because it yields parts of superior quality.

The draping process consists of picking up a flat ply and conforming it to a mold surface. The governing deformation mode that allows the ply to undergo a deformation from flat to double curved is known as trellising or fabric shearing. This shearing entails, as seen in Figure 2, that the fiber tows in the weave rotate at their crossover points such that the angles change from the initially 90°. Notice, therefore, that the draping process is not simply a pick-and-place operation.

The amount of shearing necessary for a given draping process mainly depends on the curvature of the mold. The amount of shearing that can be realized with the fabric depends on several factors, of which the fabric architecture, e.g. weave pattern and tow spacing, is highly important. At a certain degree of shear, known as the *locking-angle*, the neighboring tows start to make contact which usually entails wrinkling. Notice though, that wrinkling is a complex phenomenon that does not solely depend on the shear angle. This study focuses on low-curvature molds without sharp corners which enables the plies to be readily draped without post-treatment and without the fabric reaching the locking angle. The Gaussian curvature of the mold in this study ranges between -25 m^{-2} and 23 m^{-2}.

There are certain quality requirements to the draping process. The draped ply must conform to the mold surface without wrinkles and air pockets. Also, the boundary of the ply must follow a prescribed boundary on the mold. The tolerances on the ply-mold alignment and boundary depend on the industry and the specific part but are usually in the order of a few millimeters.

The ply material used in this study is a woven fabric which is pre-impregnated with the resin - a *prepreg*. The resin influences the ply behavior in two ways. First, the bending stiffness of the otherwise limp fabric increases. Second, the tackiness causes the interface friction to become significant. Notice though, that the general methodology is not restricted to a particular material system.

2.1. The robot system

The concept of the new robot end effector under development is shown in Figure 3. The tool consists of an array of suction cups or *grippers* with a diameter of 40 mm. The grid in Figure 3 is 2 × 2, and this grid size along with a 3 × 2 grid is studied in this paper using a numerical approach. The tool may potentially be expanded to a higher number of grippers. The idea is that the three translational degrees of freedom for each gripper can be controlled individually. Rotations about the *z*-axis, i.e. yaw, is locked, whereas the two remaining rotational degrees of freedom are free to the extent allowed by the flexible bellow. It is assumed that rotations up to 40° are achievable. The work envelope of the tool is such that a 150-mm initial spacing between the center of the grippers is appropriate. The fiber directions are parallel to the edges of the ply.

The hardware design of the tool offers great flexibility in terms of different mold geometries and ply shapes. Thus, the intended use is not mass production but instead small batches. To this end, reconfiguring the automatic draping system for a new mold-ply kit should be reasonably fast.

In a previous study by Krogh et al. [3], the prepreg material was characterized experimentally for the in-plane tension and shear and out-of-plane bending responses. This characterization was used as the basis for a nonlinear rate-dependent finite element (FE) model. While this model gives good predictions of the ply deformation field during draping it is also computationally expensive; a typical draping simulation takes in the order of hours to complete. Thus, its use in an optimization

framework would entail very long computation times. With the flexibility required for the automatic robot draping system, a faster, approximate model is desired. This need is the motivation for applying the approximate ply model based on cables to predict the mechanical behavior of the ply.

2.2. Challenges with regard to automatic draping

Automatic draping with the robot system poses some challenges. In general, there are two main issues to address: where the grippers should pick up the ply and afterwards how the grippers should move during draping, i.e. the placing of the ply on the mold surface.

With regard to where the grippers should pick up the ply, these locations could be dependent on both the ply and the mold. It might be beneficial with grippers located on the perimeter of the ply to facilitate the positioning of the ply boundary. Another concern could be to have as much of the suction area as possible covered by the ply. On the other hand, certain characteristics on the mold, such as high curvatures or concave regions, might make some gripper touchdown locations more favorable than others. In this study, a rectangular ply is considered and thereby the grippers on the robot system will be arranged in a rectangular grid during pick-up. The determination of optimal pick locations in terms of the mold and non-rectangular plies is left for a future study.

The remaining issue is how the grippers should move during draping. As an aid, the final locations of the grippers on the mold or *target points* can be predicted using a kinematic mapping algorithm [16]. The basic idea is to preserve the fabric length in the fiber directions on the mold while allowing shearing. Details of the calculation of the target points can be found in Krogh et al. [3].

With the above challenges in mind, the task is to determine the path from the initial position of the grippers to their respective target points by means of optimization. Without making any limiting decisions a priori, one possible parameterization would be to employ interpolating functions, for instance splines as shown in Figure 4. Here, it is envisioned that a number of control-point design variables define splines which will determine the trajectory of a gripper together with the corresponding velocity profile. The objective function to be minimized could be a *drape quality measure* involving the mold-ply distance for the draped ply. Hereby, an objective function evaluation necessitates a simulation of the entire draping sequence. The control points are updated until the drape quality measure is sufficiently low.

Another idea is to take a more heuristic approach, employing information from manual layup. Here, the operator tends to choose some initial contact or *seed point* from where the ply is draped in an incremental manner. The contact front thus advances away from the seed point in a manner where the movement of the ply mimics a wave. This motion is continued until the entire ply is draped. This drape motion helps to mitigate wrinkles and issues with entrapped air that occur due to bridging.

A parameterization based on the heuristics of manual layup is depicted in Figure 5. The draping of the ply is divided into iterations. In each iteration, an optimization problem is solved where the design variables are the gripper positions, and the objective is to bring the ply closer and closer to a draped configuration. Careful choice of optimization criteria will generate the wave-shaped drape motion. Move limits are imposed to make sure the grippers travel in small increments. Then, a call to the objective function only requires an evaluation of the ply model in a single gripper configuration. When all the grippers eventually make contact with the mold, the process is terminated, and the locus of the incremental positions of a gripper constitute its trajectory.

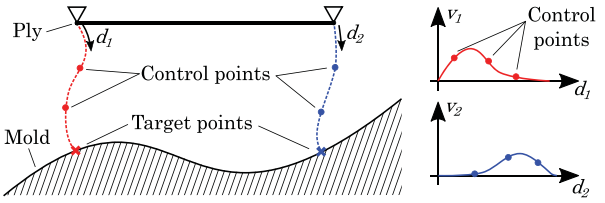

Figure 4. Possible parameterization of gripper trajectories (d_1 and d_2) and velocity profiles (V_1 and V_2) using splines.

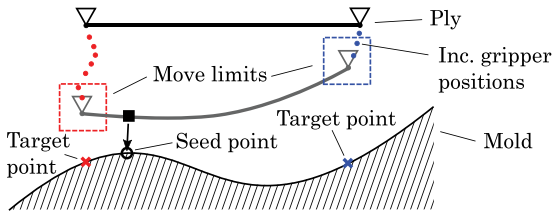

Figure 5. Parameterization using incremental optimization with inspiration from manual layup.

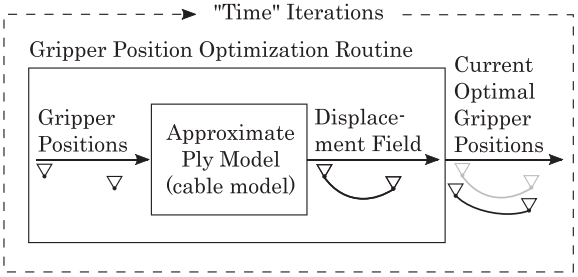

Figure 6. Flowchart of the incremental optimization scheme. "Time Iterations" denote the iterations in which the discrete trajectory points are obtained.

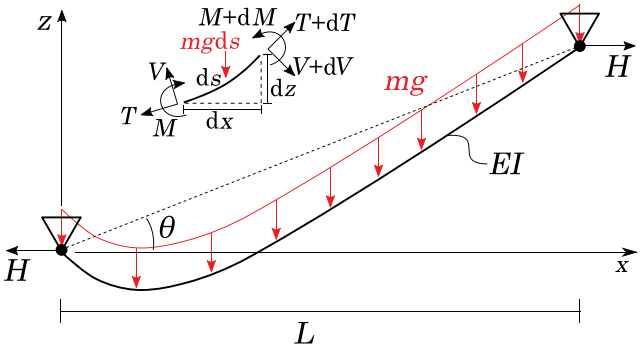

Figure 7. Free body diagram of cable with bending stiffness [18].

Due to the well-proven wave-shape drape motion and the fact that the incremental optimization scheme is more computationally efficient than the spline-inter-polation scheme, it is employed in the present study. A flowchart of the gripper optimization process is presented in Figure 6.

3. The cable model

The key concept of the approximate model is to suspend cable curves between the center points of the grippers. By this simplification, the actual gripper geometry is ignored in the model. The material properties are chosen to be linear elastic for computational efficiency. The following gives an overview of the model and details can be found in Krogh et al. [17].

3.1. 2D Cables

The basis of the model is a 2D inextensible cable with bending stiffness or more generally, an *Euler elastica*. Accounting for large rotations, the force equilibrium on the infinitesimal cable segment in Figure 7 can be used to set up a nonlinear differential equation [18]. In the figure, H is the horizontal component of the cable force T and M and V are the bending moment and shear force, respectively. EI is the flexural rigidity, and mg is the *weight per unit length*.

Assuming small sag (less than 1/4 of the span) such that the gravity load can be assumed uniformly distributed between the support points and also a linear curvature definition, a linearization can be carried out [19]. The linear differential equation becomes:

$$Hz''(x) - EIz''''(x) = \frac{mg}{\cos(\theta)} \tag{1}$$

Here θ is the tilt angle between the support points. A closed form solution can be obtained which predicts the z-coordinate of the cable as function of the x-coordinate, the material properties EI and mg, but also the horizontal component of the reaction force, H. Thereby, the arc length of the cable does not explicitly enter into the solution but rather, it depends on H. This matter is addressed later in this section.

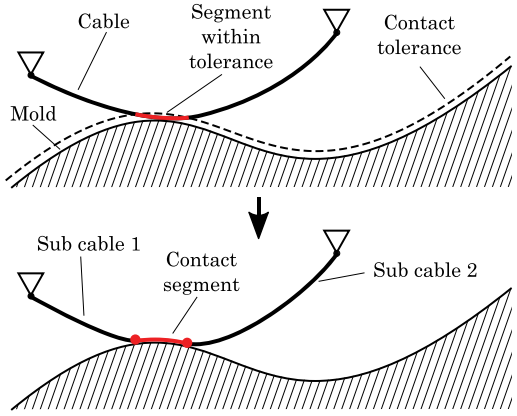

Figure 8. Contact formulation for cable model. Left: segment of cable is within contact tolerance. Right: contact segment is fixed and two sub cables are created.

Two different boundary conditions are used for the cable end points depending on the gripper to which it is attached: either a zero moment ($z'' = 0$) or a prescribed slope ($z' = s_{pre}$). The former is used with grippers attached to free ends of the ply where the slope is free. The latter is used to ensure C^1 continuity when multiple cables attach to the same gripper in the interior of the ply. Here, the value of s_{pre} needs to be determined. The prescribed slope boundary condition is also used to enforce the maximum gripper rotation of 40°.

The above description leaves two families of unknown variables for the model to be determined: the horizontal components of the reaction forces H and the prescribed slopes for shared grippers, s_{pre}. This determination is achieved by a minimization scheme, where the arc lengths of the cables are constrained to their prescribed lengths and the sum of squares of the reaction forces are minimized. Details can be found in Krogh et al. [17].

An advantage of the cable model is that it can easily be split into segments as mold contact occurs. The contact formulation employed is outlined in Figure 8. A contact tolerance with respect

to the mold surface is specified. In each iteration of the draping process, possible contact is evaluated. That is, if a portion of a cable is within the specified tolerance, that portion is considered in contact with the mold. Thereafter, it will be fixed on the mold surface and two independent sub cables are created. This contact formulation corresponds to an infinite friction condition which can be justified for the current material system by the tackiness of resin.

3.2. A preliminary numerical result highlighting the challenges

By means of a 2 D cable model with three grippers, the challenges with regard to trajectory generation pointed out in Section 2.2 can be demonstrated. Consider a 160-mm long ply with the gripper attachment points located at the left end, halfway and at the right end of the ply. The initial gripper points have z-coordinates of 60 mm and x-coordinates of 5 mm, 80 mm and 155 mm, respectively. This configuration corresponds to the topmost gray dashed line (It. 1) in Figure 9. The mold definition is provided in Appendix A. The first target point is located at an x-coordinate of 5 mm, i.e. directly below the starting point of the leftmost gripper. The second and third target points are located 80 mm and 160 mm away, respectively, along the arc length of the mold. Notice, that the target points preserve the ply length on the mold surface. For this 2 D example, the material properties are chosen to be $EI = 10^{-5}$ Nm^2 and $mg = 12$ N/m as it was found to provide a reasonable output. Material properties for the 3 D cable model are treated in further detail in Section 3.4.

The grippers are moved by means of simple trajectories (black dots in Figure 9) created as linear interpolations between the initial position and the target point of each gripper. Thereby, the grippers will in theory reach their target points, but as is evident from the following, it does not necessarily lead to an acceptable draped configuration. The ply is shown in iterations 1 (initial), 12 (upon first mold contact) and 24 as gray dashed lines and in the current iteration 35 in solid red line.

Although the grippers have not yet reached their target points, two issues can be identified in Figure 9. First, the ply is not aligned on the mold with respect to the target points. For example, the distance from the leftmost target point to the leftmost mold-ply contact front is more than 3 mm larger than the corresponding free ply length. Second, two separate portions of the ply are in contact with the mold, i.e. for $x \in [12; 68]$ mm and $x \in [134; 136]$ mm, respectively. Because the arc length of the non-draped ply between the contact segments is larger than the corresponding arc length of the mold, this situation will eventually lead to a wrinkle. As a consequence, further gripper movement is meaningless in the absence of ply sliding on the mold. These defects are small but serve to illustrate the principle of an infeasible draping sequence.

3.3. 3 D Effects

As of now, only 2 D cables have been considered. When modeling a 3 D ply, some extra aspects must be taken into account. The basic idea is still to suspend cables between the grippers and in 3 D, diagonal cables are also employed as sketched in Figure 10 such that *unit cells* are created. The purpose of the diagonals is to improve the representation of the ply in the center of the unit cell and to account for *shearing* which was introduced in Figure 2. It is assumed that a unit cell behaves like a parallelogram, and the diagonals change their lengths accordingly. This behavior of the diagonals can appear counter-intuitive but notice that they do not represent actual fiber tows (See Figure 10).

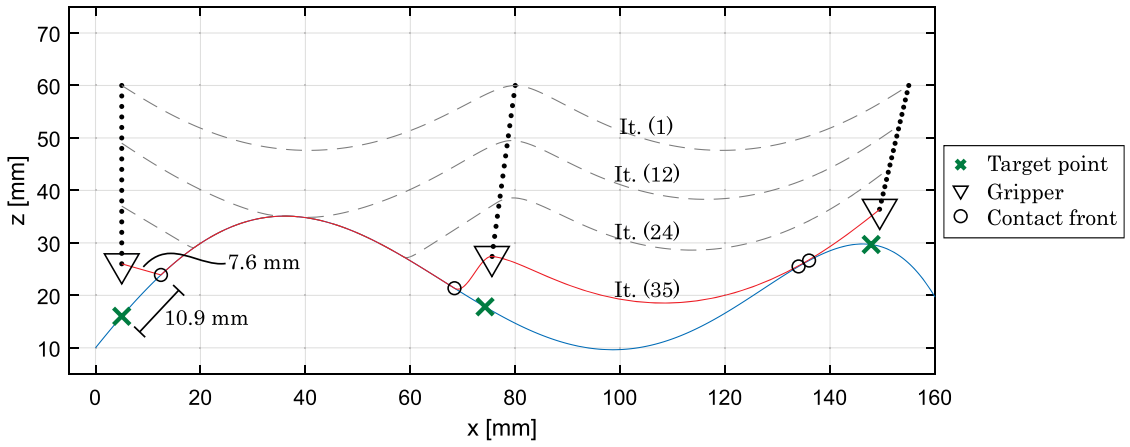

Figure 9. Draping of 2 D ply onto mold with gripper trajectories prescribed as linear interpolations. The gray dashed lines show the ply in iterations 1, 12 and 24.

Suspending the two diagonals across a unit cell, i.e. letting them hang freely from their respective grippers, does not necessarily entail that they will intersect. To ensure continuity in the model, a *post-processing* approach is adopted: The idea is to keep the highest (topmost) diagonal intact while re-evaluating the lowest (bottommost) diagonal. The lowest diagonal is first split up in two half segments. Next, the half segments are re-evaluated such that each new half segment suspends between a gripper and the center point of the highest diagonal. This approach is depicted in Figure 11.

3.4. Cable model material data

The ply material has a thickness and areal mass density of 0.3 mm and 314 g/m^2, respectively. The force-elongation response in the various deformation modes, i.e. fiber direction tension, in-plane shear and out-of-plane bending are nonlinear and rate-dependent. Here, the response is modeled as linear elastic.

The 2 D cable model is based on the physical quantities "flexural rigidity" and "weight per unit length", but it is not obvious what values these parameters should assume. Both can be related to material properties and geometrical parameters, but this connection is not clear when the cables are assembled into 3 D unit cells. Therefore, it was decided to use a least squares approach to match the cable model with a linear elastic FE model which is based on input from material tests [20]. Two compression tests with different out-of-plane rotation boundary conditions were simulated for a unit cell which yielded maximum deflections of approximately 29 mm. By considering the difference in the predicted displacement fields, EI and mg for the cable model were determined to $EI = 9 \cdot 10^{-5}$ Nm^2 and $mg = 12.26$ N/m. The norm of the residual vector was $3 \cdot 10^{-2}$ mm.

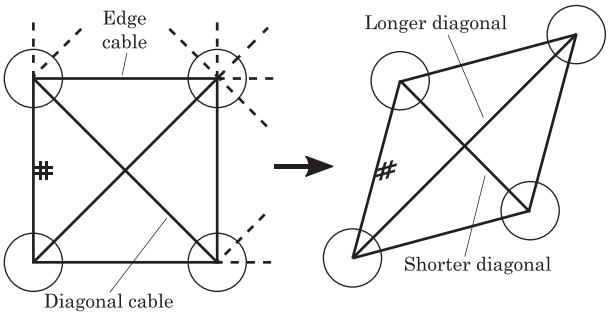

Figure 10. Assembly of cables into unit cells which can undergo shearing. Grippers are shown as circles but do not have any physical extent in the model. Fiber angles are indicated at the left edges.

3.5. Behavior in compression

Equation (1) is a differential equation of a general nature which allows the value of H (horizontal component of the reaction force) to assume both positive and negative values. When H is positive, corresponding to tension, the cable solution predicts a parabola-shaped sag (see the left of Figure 12), where a lower value of H equals more sag. On the other hand, if H goes towards infinity, the cable solution will approach a straight line between the supports.

In compression, i.e. with H negative, the response is quite different. In fact, it corresponds to a buckling problem where multiple solutions, i.e. buckling modes, can have the same cable arc length. Upon comparing Equation (1) to the differential equations that are used to study buckling of Euler columns and beam-columns, it can be seen that they take the same form [21]. A cable with multiple solutions yielding the same length of 150 mm is illustrated in Figure 13.

The fact that multiple solutions have the same length causes some issues when evaluating the cable model. In practice, higher modes are not physical

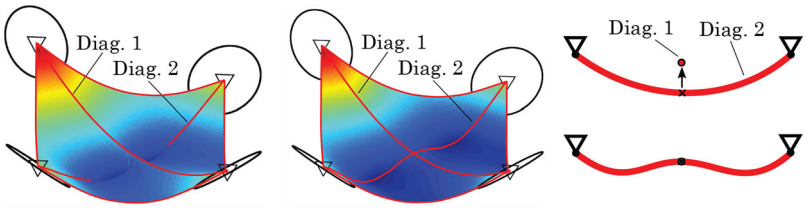

Figure 11. The postprocessing approach for ensuring continuity with the diagonals. Left: before postprocessing. Center: after postprocessing (diagonals are coincident). Right: 2 D view of postprocessing.

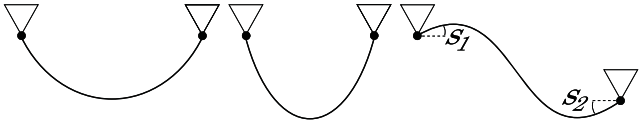

Figure 12. Different shapes of cable solutions. Left: cable under tension ($H > 0$). Middle: cable under compression (1st buckling mode, $H < 0$). Right: cable under compression with prescribed slopes (2nd buckling mode, $H < 0$).

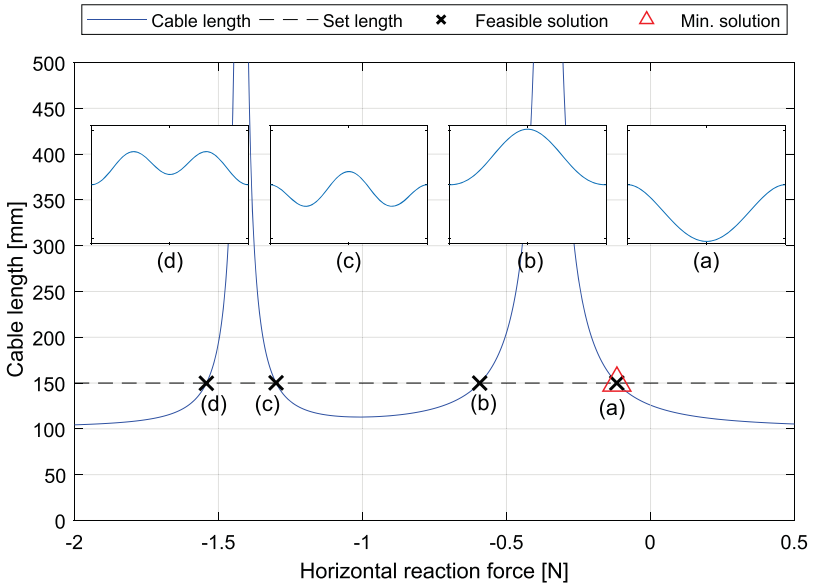

Figure 13. Cable length vs. horizontal reaction force for cable with 100 mm span and fixed end point rotations. Four values of the reaction force yield the sought length of 150 mm. The peaks located at -0.355 N and -1.42 N correspond to the singularities in the differential equation.

because they correspond to unstable equilibria. Nevertheless, some buckling modes must be considered in the model. For instance, if endpoint slopes S_1 and S_2 are prescribed as in the right of Figure 12, the 2nd buckling mode can be a quite realistic configuration.

To limit the number of possible length solutions, the critical loads, i.e. reaction forces that produce buckling can be determined and used as the lower bounds for the reaction forces in the cable model. The first critical load suffices in many cases but as stated above, the second critical load can also come into play. If the length of the cable computed with the first critical load is smaller than the prescribed length, then the second critical load must be used as the lower bound. This situation would be the case for the configuration to the right in Figure 12.

For determining the critical loads, the classical Euler solutions are valid due to the similarity of the differential equations as noted above. The critical load H_{cr} depends on the mode number and the boundary conditions, but the equation takes the general form [21]:

$$H_{cr} = \frac{\alpha\ \beta\ \pi^2 EI}{L^2} \tag{2}$$

The values of α (mode number dependent) and β (boundary condition dependent) are given in Table. 1. The flexural rigidity EI was determined in Section 3.4, and the length L, as seen in Figure 7, is the horizontal length between the supports. The reason why, the horizontal length must be used is that the differential equation for column buckling is derived for a straight column in the undeformed configuration, where the force is likewise parallel to the column. By using Equation (2) for the problem in Figure 13, the critical reaction forces are predicted to be -0.355 N and -1.42 N respectively, which are identical to the values determined from the graph.

Table 1. Parameters α and β used in the Euler buckling Equation (2) [21].

	Free-Free	Fixed-Fixed	Free-Fixed
1st mode	$\alpha = 1^2$	$\alpha = 1^2$	$\alpha = 1$
	$\beta = 1$	$\beta = 4$	$\beta = 2.046$
2nd mode	$\alpha = 2^2$	$\alpha = 2^2$	$\alpha = 2.72$
	$\beta = 1$	$\beta = 4$	$\beta = 2.046$

4. Optimization setup

This section presents the optimization setup used for generating gripper trajectories. The criteria used for the incremental optimization approach from Figure 5 are elaborated. The algorithm used for the optimization is the *SQP* (Sequential Quadratic Programming) from MATLAB's built-in function *fmincon*. This algorithm was chosen for its ease of implementation. In principle, any gradient-based optimization algorithm would work.

4.1. Optimization criteria

The purpose of the optimization criteria is to guide the ply during draping in a manner which resembles manual layup as discussed in Section 2.2. The observations from the preliminary 2 D example in Section 3.2 provide useful information as well. In the following, the optimization problem and criteria are presented in 2 D and additions applicable to 3 D are explained afterwards.

The draping sequence is split up into two parts: before mold contact and after mold contact. The

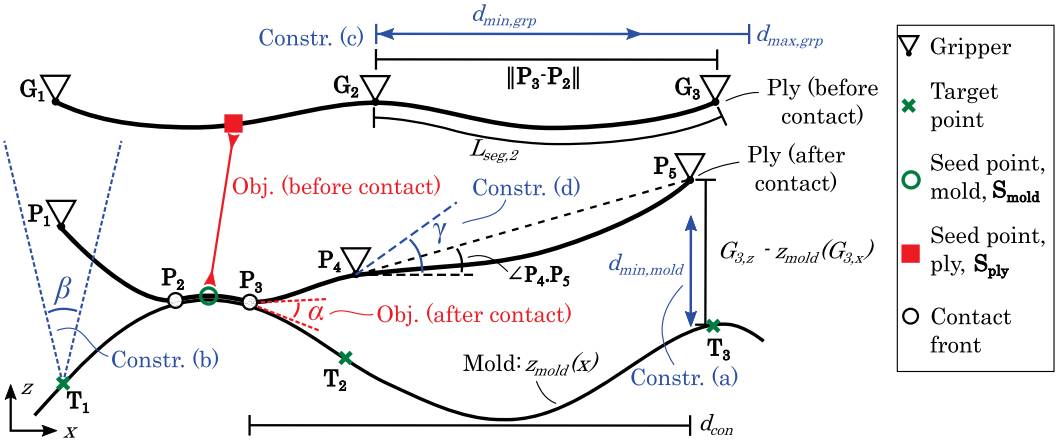

Figure 14. Graphical representation of objectives and constraints in optimization setup. For ease of viewing, each criterion is only shown once, but e.g. "Constr. (b)" applies for all target points.

former concerns the proper alignment of the ply using a seed point such that the ply border will eventually match the boundary. The latter concerns the wave movement where the ply is draped in directions away from the seed point.

From the 2 D example in Figure 9, it can be seen that the first mold-ply contact occurs at the highest point on the mold. This result makes sense because the ply is sagging. With this result in mind, a natural choice for the seed point on the mold, $\mathbf{S_{mold}}$, would indeed be the highest mold point. The corresponding point on the ply, $\mathbf{S_{ply}}$ which is to reach the mold seed point, can then be determined based on preservation of ply arc length on the mold. Thereby, the first objective is to minimize the distance between the aforementioned points. This criterion is depicted as "Obj. (before contact)" in Figure 14. Notice, that any point on the mold could be chosen as the seed point.

Next, to advance the draping, the portions of the ply near the contact fronts are considered. Specifically, the angle between the mold and the ply in the contact fronts, α_i, are minimized. This criterion corresponds to "Obj. (after contact)" in Figure 14.

The issue highlighted in the 2 D example (Figure 9) was multiple contact segments of the ply, which in general is likely to result in either wrinkling or bridging. In the optimization, it is alleviated by forcing the part of the ply which is not in proximity of the current contact fronts to remain some distance above the mold. Thereby it can be assured that only one contact segment will exist during draping. The constraints are implemented at the grippers, and the minimum distance above the mold is denoted $d_{\text{min, mold}}$, which is dependent on the distance to the contact point, d_{con} (elaborated later in the section). This condition is shown as "Constr. (a)" in Figure 14.

To add robustness (and alignment during draping in 3 D) an additional family of constraints is specified. "Constr. (b)" in Figure 14 forces each gripper to remain inside an inverted triangle (cone in 3 D) with the apex located at the corresponding target point. The criteria mentioned above serve to control the draping of the ply. In addition some criteria are implemented to keep the ply behavior within its physical limits:

- Penalization of mold-ply penetrations added as a term, Φ, to the objective function. Φ is a sum of all penetration distances.
- Constraints on the maximum and minimum distance between adjacent edge cable grippers. Because the fabric is virtually inextensible in the fiber direction, gripper sliding could occur in practice, if the gripper distance exceeds the segment length. Also, if the gripper distance is too small, excessive sagging will occur which violates the cable model assumptions. This family of constraints is exemplified as "Constr. (c)" in Figure 14.
- Constraints on the maximum inclination angle between adjacent edge cable grippers as seen in "Constr. (d)" in Figure 14. These constraints serve to avoid extreme gripper positions which cannot be achieved by the robot tool.

The design variables of the problem, i.e. the gripper positions, are collected in the vector $\mathbf{G} = \{x_1, z_1, \ldots, x_{nGrp}, z_{nGrp}\}^{\mathrm{T}}$ where $nGrp$ denotes the number of grippers. For convenience, a double index notation is introduced where the first index $(1, \ldots, nGrp)$ denotes the gripper number and the second index (x, z) denotes the coordinate. Thus, $G_{2,x}$ corresponds to the x-coordinate of the 2nd gripper. On the other hand, if only the first index is specified, e.g. $\mathbf{G_j}$, the resulting quantity is the vector of coordinates for the jth gripper.

When contact occurs, cables will be suspended between the contact fronts and the grippers as

sketched in Figure 8. The cable end points are thus obtained by augmenting **G** with the contact front points, whereby the vector **P** is obtained. Notice that **G** and **P** are equivalent before contact. The double index notation is also applied to **P** and the vector of target points **T**. The optimization problem is formulated as follows:

$$\begin{aligned}
\min_{\mathbf{G}} \quad & \overbrace{||\mathbf{S_{mold}}-\mathbf{S_{ply}}||}^{\text{Before contact}} \quad \text{OR} \quad \overbrace{\sum_{i=1}^{nCon}\alpha_i}^{\text{After contact}} \quad + \Phi \\
\text{s.t.} \quad & (a)\ G_{j,z}-z_{\text{mold}}(G_{j,x}) \geq d_{\text{min, mold, j}} \\
& (b)\ |G_{j,x}-T_{j,x}| \leq (G_{j,z}-T_{j,z})\tan\left(\frac{\beta}{2}\right) \\
& (c)\ d_{\text{min, seg, }k} \leq ||\mathbf{P_{k+1}}-\mathbf{P_k}|| \leq d_{\text{max, seg, }k} \\
& (d)\ |\angle \mathbf{P_k}, \mathbf{P_{k+1}}| \leq \gamma \\
& \forall j\ ,\ j = 1, \ldots, nGrp \\
& \forall k\ ,\ k = 1, \ldots, nSeg
\end{aligned} \tag{3}$$

Here *nCon*, *nGrp* and *nSeg* are the number of contact fronts, number of grippers and number of cable segments, respectively, Φ is the mold-ply penetration penalty, and β and γ are the target point triangle and gripper inclination constraint angles, respectively (See Figure 14). The quantity $d_{\text{min, mold, j}}$ from constraint (a) is calculated as follows:

$$d_{\text{min, mold, }j} = \min(d_{\text{con, }j}c_{\text{dist, mold}}\ ,\ c_{\text{sat, mold}}) \tag{4}$$

Thus, the vertical distance that the *j*th gripper must keep to the mold is its distance to the contact front $d_{\text{con, }j}$ (see Figure 14) scaled by a parameter $c_{\text{dist, mold}}$. Further, a saturation value of $c_{\text{sat, mold}}$ is specified. The quantities $d_{\text{min, seg, k}}$ and $d_{\text{max, seg, k}}$ in constraint (c) are calculated as follows:

$$d_{\text{min, seg, }k} = c_{\text{min, seg}}L_{\text{seg, }k} \tag{5}$$

$$d_{\text{max, seg, }k} = c_{\text{max, seg}}L_{\text{seg, }k} \tag{6}$$

Thus, the grippers must remain within a distance of each other defined by the segment arc length L_{seg} and two scaling parameters $c_{\text{min, seg}}$ and $c_{\text{max, seg}}$ which naturally must be defined according to $0 \leq c_{\text{min, seg}} \leq c_{\text{max, seg}} \leq 1$.

Notice that this formulation of constraints is efficient because it does not require the evaluation of the ply model. That is, the constraints only operate on **P**. Common to all constraints is that they vanish when either the distance between a particular gripper and its target point or the length of the cable segment attached to the gripper is less than a tolerance, L_{tol}. The exception is constr. (c) where the parameter $c_{\text{max, seg}}$ is relaxed to unity. This unity state implies, that the corresponding cables are allowed to be fully stretched.

For 3 D optimization problems, another horizontal coordinate, *y*, is included. Regarding the choice of seed point, the highest mold point is not a robust option because the corresponding point on the ply might not be defined. That is, the ply is only defined at the cables. Therefore, in 3 D, the grippers and their corresponding target points are considered as possible seed points. Specifically, the highest target point that is also in a direction of shear on the mold is chosen. Mold contact of the seed point gripper will mark the transition to the wave motion draping.

In addition, the 3 D alignment of the ply now requires more than just the seed point. For this purpose, the (up to four) grippers connected to the seed point gripper by edge cables, will act as "alignment grippers". Before contact of the seed point gripper, an alignment term is added to the objective function. This term is the sum of the horizontal distances between each alignment gripper and a line connecting the seed point with the target point of the corresponding alignment gripper.

Finally, shearing during alignment of the ply is not desired which is why it is penalized in the objective function before contact of the seed point gripper. After contact, a large difference between the diagonal gripper distances can cause sagging of one diagonal cable, e.g. as shown in Figure 11. This sagging is mitigated by a penalization term added to the objective function when the vertical distance between the diagonal crossover point and the mold surface is less than a tolerance, $c_{\text{diag, sag}}$.

This section has presented an elaborate optimization scheme with a number of parameters whose values must be specified. To this end, it should be noted that all parameters have a physical meaning and that some parameters, e.g. γ, can be determined based on the specifications of the robot tool.

5. Numerical results

This section presents numerical results with the cable model. Mold definitions can be found in Appendix A. For visualization purposes in the 3 D models, the grippers are drawn as circles, and a surface is interpolated in the unit cells, where the colors scale with the *z* coordinate. For the optimization examples, some common settings are given in Table 2. These settings are believed to be generally applicable.

Table 2. Common optimization settings for all examples in Section 5. *ConTol* and *GrpTol* are the ply and gripper contact tolerances, respectively.

ConTol [mm]	*GrpTol* [mm]	$c_{\text{sat, mold}}$ [mm]	$c_{\text{max, seg}}$ [-]	γ [°]
0.3	0.35	50	0.99	35

5.1. 2 D Optimization example

Recall the 2 D example from Section 3.2 and Figure 9 where a linear interpolation was employed as the trajectory for each gripper. This simple draping strategy resulted in multiple contact segments and possibly wrinkling. Consider now the same setup, but with the difference that the optimization scheme described previously is used to determine the trajectories of the grippers. The result is shown in Figure 15. From this figure, it can be seen that the ply is draped in a wave movement as desired. Only one contact segment exist throughout the draping and the grippers are within half a millimeter of their respective target points in the draped configuration. The optimization settings used for this result are provided in Table 3.

5.2. Validation of 3 D cable model

As a validation of the cable model and in particular its ability to account for shearing, consider the example in Figure 16. The example is a comparison between the cable model and the non-linear rate-dependent FE model from Krogh et al. [3]. The latter will be the baseline for the comparison. The setup concerns draping of a 300 mm by 150 mm ply onto a flat parallelogram-shaped mold where the mold shear angle is 20°. The gripper trajectories are prescribed linear interpolations from the initial gripper positions to the respective target points. The draping time is 10 s, which is a reasonable time for the robot system. Recall though, that the cable model is time-independent.

Figures 16(a) and (b) show the initial configurations with the ply suspended 40 mm above the mold and with gripper (1,1) located directly above its target point. The initial grid spacing of the 300 mm by 150 mm ply is 148 mm which is why both models exhibit sag. The deformation field is slightly different between the two models, and this difference is a result of the difference between the gripper boundary conditions in the respective models. However, the maximum vertical displacement is only overpredicted by 2.5 mm by the cable model. Figures 16(c) and (d) present the results at 10% of the draping sequence. The ply is now beginning to shear while there is still some slack in the fiber directions. This shearing induces the diagonal waves. Finally, Figures 16(e) and (f) present the results at 75% of the draping sequence. The diagonal waves are now more distinct than at the 10% state. Due to these waves, both models predict small diagonal wrinkles in the draped configuration. Based on the comparison of the two models, it is concluded that the cable model can give predictions of the displacement field of the ply during draping that are comparable to the FE approach.

5.3. 3 D Optimization Example 1

The first 3 D example is shown in Figure 17 and involves a grid of 2×2 grippers draping a ply onto a region of the mold surface with low and primarily convex curvature. In this region, the minimum positive and negative radii of curvature are 320 mm and -148 mm, respectively. The initial configuration is

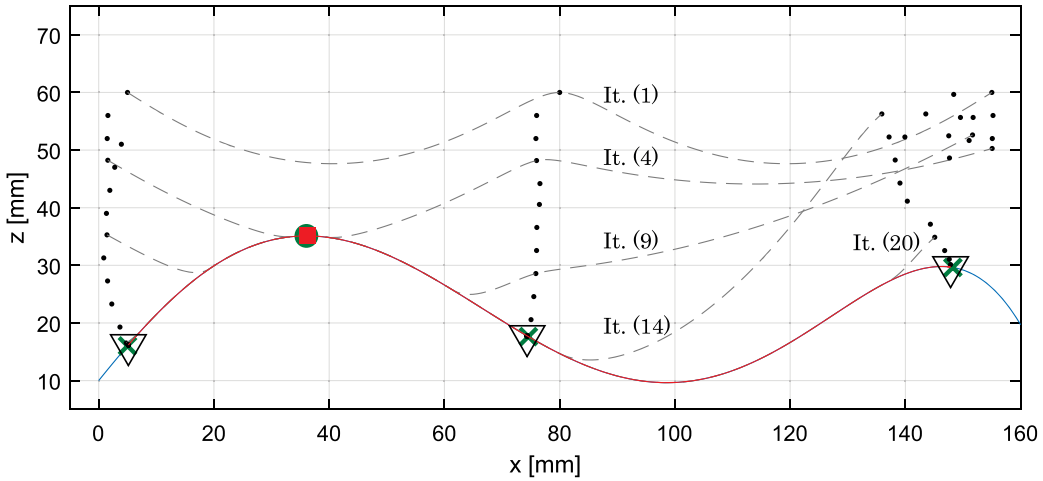

Figure 15. Draping of 2 D ply onto mold with gripper trajectories generated from optimization. The gray dashed lines show the ply in iterations 1, 4, 9, 14 and 20. The red line shows the ply in the final iteration 24.

Table 3. Optimization settings used for 2 D example in Figure 15. ΔG is the move limit per iteration.

L_{tol} [mm]	ΔG [mm]	$c_{dist,\,mold}$ [-]	$c_{min,\,seg}$ [-]	β [°]
10	±4	0.2	0.93	70

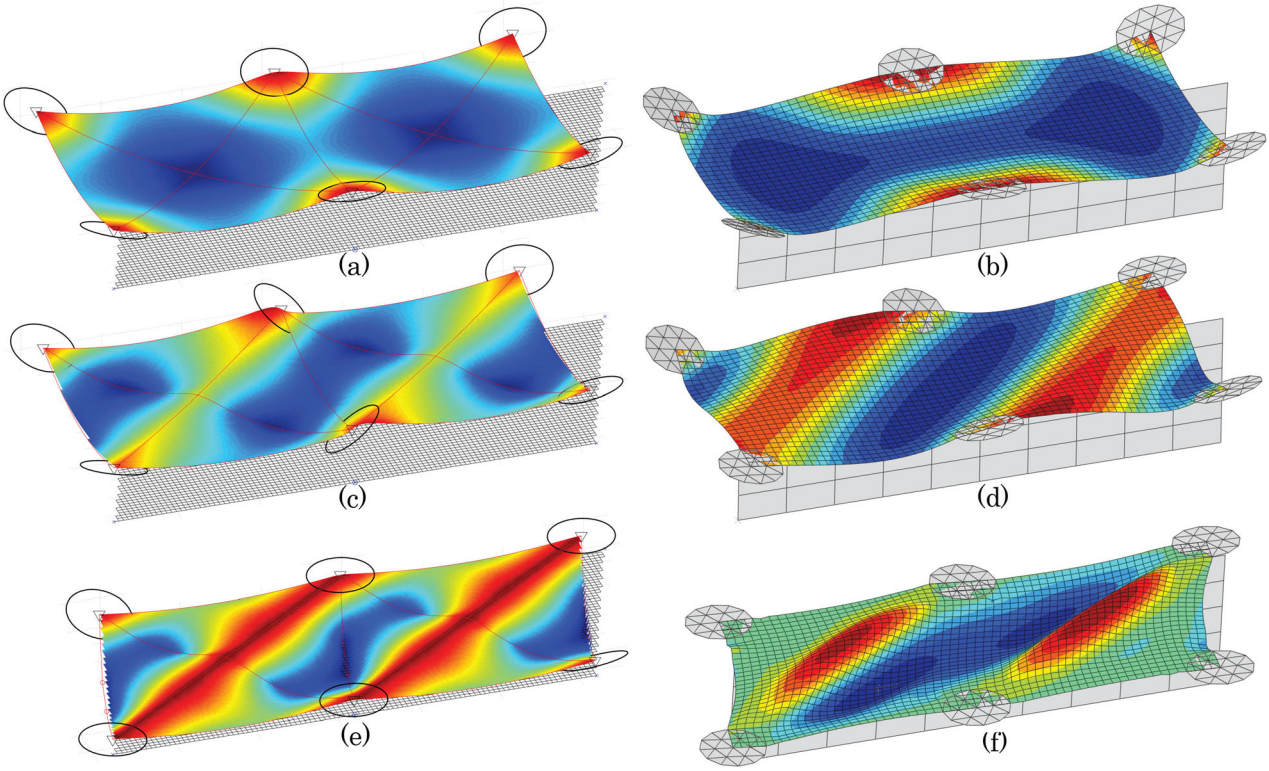

Figure 16. Draping onto flat parallelogram mold with cable model ((a), (c) and (e)) and FE model ((b), (d) and (f)). The rows correspond to the initial configuration, 10% done and 75% done respectively.

presented in Figure 17(a) where the seed point gripper (1,1) is located 50 mm above its target point. Contact with the seed point is established in Figure 17(b) and hereafter the drape movement follows a wave in a direction towards gripper (2,2) as seen in Figure 17(c)–(f). In the draped configuration the ply is positioned such that the grippers are within 1.8 mm of their target points. The optimization settings used for this example are provided in Table 4. The computation time was 26 min on an ordinary laptop. It is believed that this time could be lowered with a more efficient implementation.

5.4. 3 D Optimization Example 2

The second 3 D example is presented in Figure 18 and involves a grid of 3×2 grippers. In this example, the chosen region of the mold has a higher curvature than in 3 D Example 1 with the minimum positive and negative radii of curvature equal to 175 mm and -144 mm, respectively. In addition, it is a more difficult problem than 3 D Example 1 because it contains convex and concave regions. In Figure 18(a), the ply is in the initial configuration with the seed point gripper (2,1) located 50 mm above the seed point, and in Figure 18(b) the seed point gripper has reached the mold surface. Figures 18(c)–(e) present three intermediate iterations where the grippers in the left unit cell progressively make contact with the mold. Figure 18(f) is the final draped configuration where the grippers are located within 2 mm of their target points. The ply is in contact with the mold surface everywhere except for the concave region near gripper (3,2). Here the ply is bridging with a maximum distance to the mold of 3 mm. This issue of bridging is revisited in the Discussion section. The optimization settings are the same as in the previous example, i.e. as given in Table 4. For this example the computation time was 2 h on an ordinary laptop.

6. Discussion

The results in the preceding section show promise in terms of generation of feasible gripper trajectories. The quality requirement of close conformity to the mold surface was, however, not fulfilled in the second 3 D example (Figure 18). A number of remedies to this situation exist. Because the bridging portion of the ply is in a diagonal direction, the ply can be stretched locally *via* an increase in shear. Therefore, the bridging portion could maybe be put onto the mold by means of a push from a gripper subsequent to draping. Another solution would be to use a smaller grid spacing or, if the grid is non-rectangular, make sure that a gripper is located in this particular spot on the mold. A final solution is to pre-shear the ply which could be achieved either when the ply has been picked by the robot or in a preceding operation.

The optimization approach presented in this study involves some settings that define the

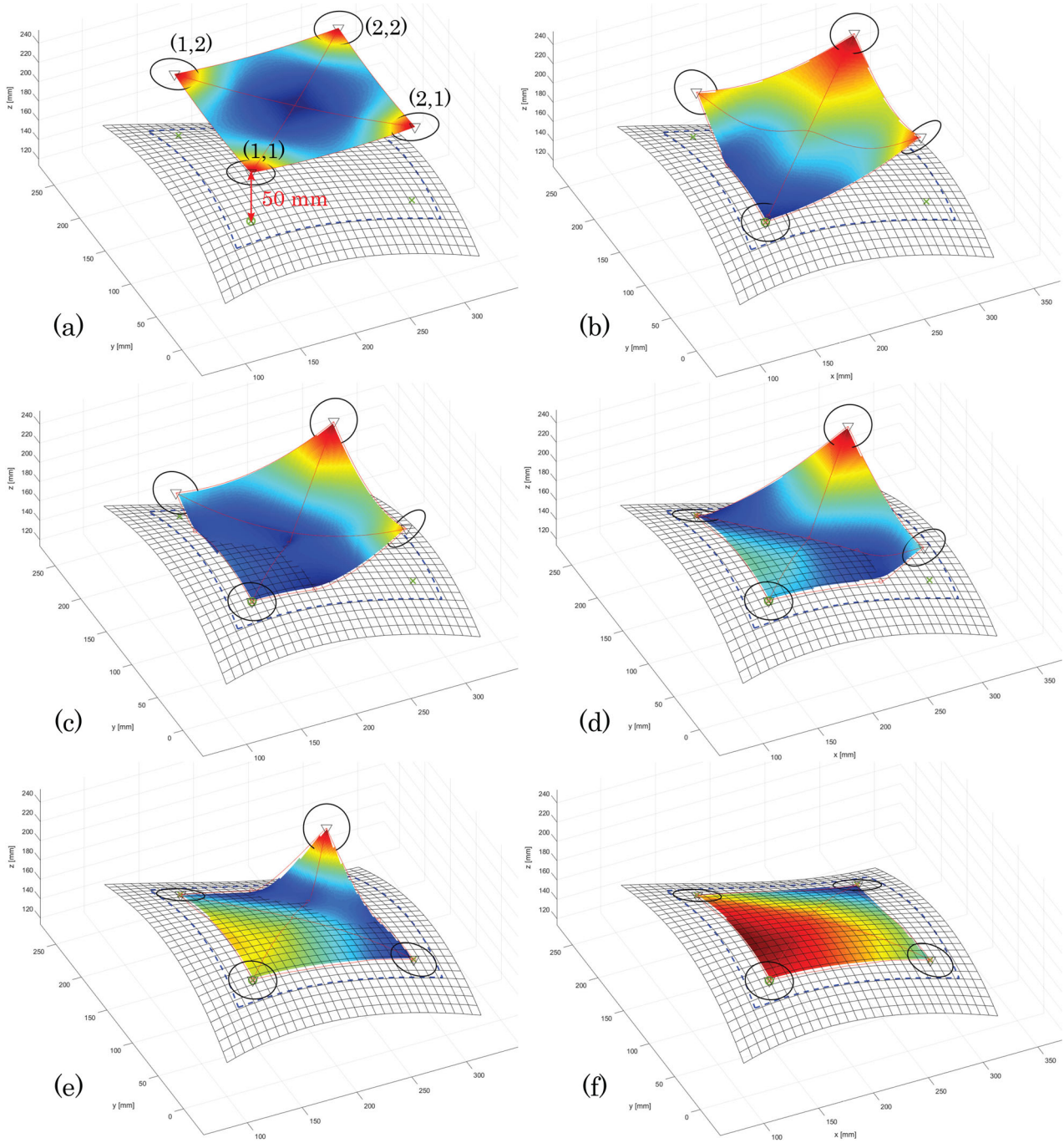

Figure 17. Draping of ply with a 2×2 gripper grid onto mold. Iterations 1, 12, 17, 26, 34 and 56 are presented in (a)-(f). The blue dashed line indicate the prescribed boundary.

Table 4. Optimization settings used for 3 D examples in Figures 17 and 18. ΔG is the move limit per iteration.

L_{tol} [mm]	ΔG [mm]	$c_{dist,\,mold}$ [-]	$c_{min,\,seg}$ [-]	β [°]	$c_{diag,\,sag}$ [mm]
20	±5	0.25	0.96	35	15

"tightness" of the constraints. To that end, some degree of tuning could be necessary when considering a new draping problem. Yet, the settings have a direct physical meaning which aids the process. For instance, if multiple contact segments develop during draping, the parameter $c_{dist,\,mold}$ from Equation (4) must be increased. In a future study, it could be investigated if the settings can be changed adaptively during the iterations: with the occurrence of multiple contact segments, the program can jump back a few iterations, change settings and then continue.

Other improvements to the present implementation include the use of a cable model accounting for large displacements and curvatures as well as having the ability to model non-rectangular ply shapes. For the former, an increase in computational time is expected which must be assessed with regard to the

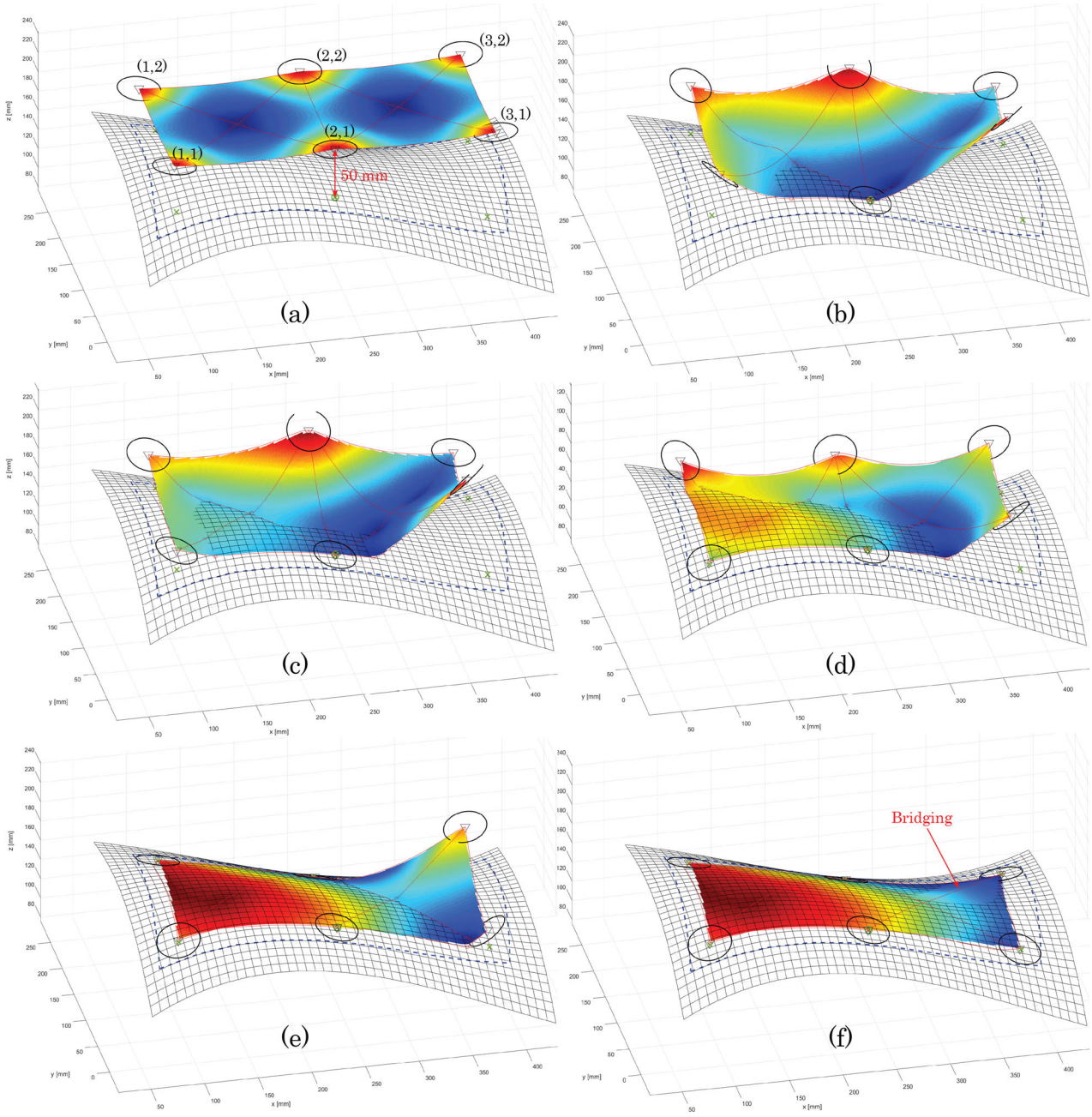

Figure 18. Draping of ply with a 3×2 gripper grid onto mold. Iterations 1, 13, 23, 36, 47 and 60 are presented in (a)-(f). The blue dashed line indicate the prescribed boundary.

increase in accuracy. The latter is important for implementation in an industrial context.

Lastly, an interesting discussion is that of optimal vs. feasible gripper trajectories. Even though optimization is utilized in this study, it is far from certain that the generated gripper trajectories are optimal. Of course, "optimality" would have to be precisely defined. Nonetheless, because the optimization is merely used to incrementally fulfill the defined criteria and the problem is path dependent, the combined trajectory is likely not to be optimal.

7. Conclusion

This paper has presented an approach to generation of feasible gripper trajectories for an automatic prepreg draping system. The grippers of the robot end effector can be controlled in the three translational degrees of freedom, and these movements must be determined such that the draped ply conforms closely to the mold surface and is placed inside a prescribed boundary.

The study takes as its point of departure an approximate ply model based on cables suspended between the grippers. The cable model is able to take large deflections, mold contact and fabric shearing into account. The cable model was validated against a non-linear rate-dependent finite element (FE) model based on material test data. It was concluded that the cable model can predict the ply displacement field nearly as well as the computationally more expensive FE model.

The optimization routine is split up into two parts. First, a seed point on the ply must reach its corresponding point on the mold while ensuring proper alignment of the ply. Thereby, mold contact is established. Next, the ply is draped away from the seed point my minimizing the difference in angles between the ply and the mold in the contact fronts. Constraints are included to ensure that only one contact segment exists. This draping strategy is chosen to mimic manual layup. In addition, a number of optimization criteria are implemented to make sure that the ply is moved within its physical limits.

The numerical results show that the optimization approach can determine a draping sequence such that the quality requirements can be met. Minor misalignment and bridging was observed, but it is believed that these matters can be taken into account when transforming the output from the optimization routine to actual robot sequences. The latter is necessary when the results from this study will be validated in practice.

Disclosure statement

The authors have no conflicts of interest to declare.

Funding

The research presented in this paper is part of the FlexDraper research project. The authors wish to thank the Innovation Fund Denmark (grant no. 5163-00003B) for the funding.

ORCID

Christian Krogh http://orcid.org/0000-0003-4067-0423

References

1. Björnsson A, Jonsson M, Johansen K. Automated material handling in composite manufacturing using pick-and-place systems – a review. Rob Comput-Integr Manuf. 2018;51:222–229.
2. Gunnarsson GG, Nielsen OW, Schlette C, et al. Fast and simple interacting models of drape tool and ply material for handling free hanging, pre-impregnated carbon fibre material. In: Gusikhin O, Madani K, editors. Informatics in control, automation and robotics. ICINCO 2018. vol. 613. Lecture Notes in Electrical Engineering, Cham: Springer; 2020. p. 1–25.
3. Krogh C, Glud JA, Jakobsen J. Modeling the robotic manipulation of woven carbon fiber prepreg plies onto double curved molds: A path-dependent problem. J Compos Mater. 2019;53:2149–2164.
4. Lin H, Wang J, Long A, et al. Predictive modelling for optimization of textile composite forming. Compos Sci Technol. 2007;67:3242–3252.
5. Zhu B, Yu T, Zhang H, et al. Experimental investigation of formability of woven textile composite preform in stamping operation. Int J Mater Form. 2008;1:969–972.
6. Coutandin S, Brandt D, Heinemann P, et al. Influence of punch sequence and prediction of wrinkling in textile forming with a multi-punch tool. Prod Eng Res Devel. 2018;12:779–788.
7. Eischen JW, Kim YG. Optimization of fabric manipulation during pick/place operations. Int J Clothing Sci Tech. 1993;5:68–76.
8. Reinhart G, Ehinger C. Novel robot-based end-effector design for an automated preforming of limb carbon fiber textiles. In: Schuh G, Neugebauer R, Uhlmann E, editors. Future trends in production engineering; Berlin, Heidelberg: Springer Berlin Heidelberg; 2013. p. 131–142.
9. Molfino R, Zoppi M, Cepolina F, et al. Design of a hyper-flexible cell for handling 3D Carbon fiber fabric. In: Epureanu B, Solomon To CW, Cho HH, editors. Recent advances in mechanical engineering and mechanics. Proceedings of the 2014 International Conference on Theoretical Mechanics and Applied Mechanics (TMAM '14), Venice, Italy; 2014. p. 165–170.
10. Nagele L, Macho M, Angerer A, et al. A backward-oriented approach for offline programming of complex manufacturing tasks. ICARA 2015 - Proceedings of the 2015 6th International Conference on Automation, Robotics and Applications, Queenstown, New Zealand; 2015. p. 124–130.
11. Flixeder S, Glück T, Kugi A. Force-based cooperative handling and lay-up of deformable materials: Mechatronic design, modeling, and control of a demonstrator. Mechatronics 2017;47:246–261.
12. Eckardt M, Buchheim A, Gerngross T. Investigation of an automated dry fiber preforming process for an aircraft fuselage demonstrator using collaborating robots. CEAS Aeronaut J. 2016;7:429–440.
13. Brinker J, Prause I, Kosse P, et al. Automated handling and draping of reinforcing textiles-challenges and developments. Mech Mach Sci. 2017;46:485–493.
14. Newell GC, Khodabandehloo K. Modelling flexible sheets for automatic handling and lay-up of composite components. Proc Inst Mech Eng, Part B: J Eng Manuf. 1995;209:423–432.
15. Lin H, Clifford M, Taylor P, et al. 3D mathematical modelling for robotic pick up of textile composites. Compos Part B: Eng. 2009;40:705–713.
16. Van Der Weeën F. Algorithms for draping fabrics on doubly-curved surfaces. Int J Numer Methods Eng. 1991;31:1415–1426.
17. Krogh C, Jakobsen J, Sherwood JA.. Development of a computationally efficient fabric model for optimization of gripper trajectories in automated composite draping. EngOpt 2018 Proceedings of the 6th International Conference on Engineering Optimization; Cham: Springer International Publishing; 2019b. p. 1107–1118.
18. Hsu Y, Pan C. The static WKB solution to catenary problems with large sag and bending stiffness. Math Prob Eng. 2014;2014:1–11.
19. Irvine HM. Cable structures. Cambridge, Massachusetts: MIT Press, 1981.

20. Krogh C, Glud JA, Jakobsen J. Modeling of prepregs during automated draping sequences. AIP Conference Proceedings, vol. 1896; AIP Publishing, 2017; p. 030036.
21. Timoshenko SP, Gere JM. Theory of elastic stability. 2nd ed. New York (NY): McGraw-Hill Book Company; 1961.

Appendix A: Mold definitions

The 2 D mold surface used in Figure 9, Section 3.2 and Figure 15, Section 5.1 is given by the following 5th order polynomial:

$$z_{\text{mold}}(x) = -17113x^5 + 5413x^4 - 440x^3 - 5.45x^2 + 1.24x + 0.01 \quad (7)$$

Here $x \in [0, 0.16]$. The 3 D mold surface used in 3 D Example 1 in Figure 17, Section 5.3 and 3 D Example 2 in Figure 18, Section 5.4 is defined by a 3rd degree polynomial surface:

$$z_{\text{mold}}(x, y) = 1.004x + 1.089y - 3.667x^2 - 4.4xy - 3.75y^2 + 3.086x^3 + 8.889x^2\ y + 4.321y^3 \quad (8)$$

Here $x \in [0, 0.45], y \in [0, 0.45]$. The target points used with the mold are presented in Table A.1. The target points have been calculated using the kinematic mapping algorithm.

Table A.1. Target points for 3 D examples.

Example #	1	2
Target point 1,1	{0.1477, 0.0522, 0.1832} m	{0.0956, 0.0504, 0.1755} m
Target point 2,1	{0.2948, 0.0522, 0.1577} m	{0.2440, 0.0528, 0.1720} m
Target point 1,2	{0.1502, 0.1992, 0.1707} m	{0.1081, 0.1967, 0.1800} m
Target point 2,2	{0.2961, 0.1984, 0.1357} m	{0.2539, 0.1979, 0.1450} m
Target point 3,1	–	{0.3877, 0.0608, 0.1303} m
Target point 3,2	–	{0.4017, 0.2084, 0.1270} m